NASA TN D-7881

(NASA-TN-D-7881) COLD-AIR PERFORMANCE OF A 12.766-CENTIMETER-TIP-DIAMETER AXIAL-FLOW COOLED TURBINE. 1: DESIGN AND PERFORMANCE OF A SOLID BLADE CONFIGURATION (NASA) 23 p HC $3.25 CSCL 01A H1/02

N75-14720

Unclas 07801

COLD-AIR PERFORMANCE OF A 12.766-CENTIMETER-TIP-DIAMETER AXIAL-FLOW COOLED TURBINE

I - Design and Performance of a Solid Blade Configuration

Jeffrey E. Haas and Milton G. Kofskey

Lewis Research Center and

U.S. Army Air Mobility R&D Laboratory

Cleveland, Ohio 44135

NATIONAL AERONAUTICS AND SPACE ADMINISTRATION • WASHINGTON, D. C. • JANUARY 1975

1. Report No.	2. Government Accession No.	3. Recipient's Catalog No.
NASA TN D-7881		
4. Title and Subtitle COLD-AIR PERFORMANCE OF A 12.766-CENTIMETER-TIP-DIAMETER AXIAL-FLOW COOLED TURBINE. I - DESIGN AND PERFORMANCE OF A SOLID BLADE CONFIGURATION		5. Report Date January 1975 6. Performing Organization Code
7. Author(s) Jeffrey E. Haas and Milton G. Kofskey		8. Performing Organization Report No. E-8124
9. Performing Organization Name and Address NASA Lewis Research Center and U.S. Army Air Mobility R&D Laboratory Cleveland, Ohio 44135		10. Work Unit No. 505-04 11. Contract or Grant No.
12. Sponsoring Agency Name and Address National Aeronautics and Space Administration Washington, D.C. 20546		13. Type of Report and Period Covered Technical Note 14. Sponsoring Agency Code
15. Supplementary Notes		

16. Abstract

A solid blade version of a single-stage, axial-flow turbine was investigated to determine its performance over a range of speeds from 0 to 105 percent of equivalent design speed and over a range of total to static pressure ratios from 1.62 to 5.07. The results of this investigation will be used as a baseline for comparison with those obtained from a cooled version of this turbine.

17. Key Words (Suggested by Author(s))	18. Distribution Statement
Axial-flow turbine; Single-stage turbine; Gas turbine; Efficiency; Performance tests; Turbine cooling	Unclassified - unlimited STAR category 02 (rev.)

19. Security Classif. (of this report)	20. Security Classif. (of this page)	21. No. of Pages	22. Price*
Unclassified	Unclassified	22	$3.25

* For sale by the National Technical Information Service, Springfield, Virginia 22151

COLD-AIR PERFORMANCE OF A 12.766-CENTIMETER-TIP-DIAMETER AXIAL-FLOW-COOLED TURBINE

I - DESIGN AND PERFORMANCE OF A SOLID BLADE CONFIGURATION

by Jeffrey E. Haas and Milton G. Kofskey

Lewis Research Center and
U.S. Army Air Mobility R&D Laboratory

SUMMARY

As part of a technology program to determine the effects of cooling air discharge on the aerodynamic performance of small turbines, an uncooled solid blade version of a 12.766-centimeter-tip-diameter, single-stage, axial-flow turbine was designed, built, and tested to determine its performance over a range of speed and pressure ratios. The results of this investigation will be used as a baseline for comparison with those obtained from a cooled version of this turbine.

The turbine design point was based on driving a 10-to-1 pressure ratio compressor at a rotative speed of 70 000 rpm with a turbine inlet temperature of 1478 K. The compressor drive turbine was designed for near optimum work factor and solidity. The solid blade version of this turbine was designed for minimum tip clearance and the minimum allowable leading and trailing edge thicknesses from a manufacturing standpoint for solid blades. The resulting design had a blade number and an aspect ratio that were twice that of the cooled version. Cold-air tests were made at speeds from 0 to 105 percent of equivalent design speed and total to static pressure ratios from 1.62 to 5.07.

The results of this investigation indicated a total efficiency of 83.2 percent at both equivalent design speed and pressure ratio and equivalent design speed and work factor. This was 1.8 percentage points less than the 85 percent selected for this design.

A flow area mismatch occurred between the stator and rotor because the stator throat area was fabricated 5.5 percent undersize. A reference turbine with a similar anomaly was used to show that the performance penalty associated with this flow area mismatch would be less than one efficiency point.

INTRODUCTION

Engine performance in terms of specific fuel consumption and specific power or thrust for the small gas turbine engine in the 1.00-kilogram-per-second, 225- to 375-kilowatt class has not kept pace with that achieved in larger engines. This results from the fact that, as engine size is reduced, it becomes increasingly difficult to maintain geometric similarity with larger engines. That is, such parameters as tip clearance, aspect ratio, and trailing edge blockage must change from the optimum values established for larger engines.

To achieve high specific work in a gas turbine engine requires a high compressor pressure ratio and high turbine inlet temperature. A high compressor pressure ratio, together with the small mass flow, results in a turbine design with a small annulus area and therefore, a small blade height. High turbine inlet temperature (above 1300 K) necessitates the use of cooling air with further compromises in the stator and rotor blading (longer chord lengths and thicker blades) to provide adequate space for cooling passages and to maintain structural integrity. The longer chord lengths and smaller blade heights force the turbine towards a low aspect ratio design with a resulting efficiency penalty.

As indicated in reference 1 this efficiency penalty results primarily from increased secondary flow losses. For small blade height designs, the secondary flow fields encompass a significant portion of the airflow channel and interact in the airfoil midspan region, causing high losses. Tip clearance losses are more severe because a tip clearance of 1 to 1.5 percent of the blade height as used in larger engines is not practical in small turbines. Also, practical manufacturing tolerance limits make it more difficult to fabricate blade profiles to the same degree of accuracy achieved in larger engines. Together, these effects could reduce the level of efficiency in small turbines by five points compared with a large turbine of comparable loading, Mach number, and turning angle.

As part of the small turbine technology program at the Lewis Research Center, a two-phase program was initiated to determine (1) the baseline level of efficiency achievable and (2) the aerodynamic penalties incurred in cooling turbines in the 1-kilogram-per-second mass flow class. This program includes both axial- and radial-flow turbines. A compressor drive turbine application for a two-stage, 10-to-1 pressure ratio compressor with a mass flow of 0.952 kilogram per second, a rotative speed of 70 000 rpm, and a turbine inlet temperature of 1478 K was selected to design both an axial and a radial turbine. The single-stage axial turbine designed for this application has a 12.766-centimeter tip diameter, and near optimum work factor and solidity.

For the purpose of determining the level of achievable aerodynamic performance, a solid blade configuration was selected. A minimum tip clearance and the minimum allowable leading and trailing edge thicknesses from a manufacturing standpoint of solid blades were used. The resulting design had a blade number and an aspect ratio that were twice that of the cooled version.

This report presents the design and experimental investigation of the solid blade turbine. The experimental investigation was conducted at turbine inlet conditions of approximately 8.27 newtons per square centimeter and 300 K over a range of speeds from 0 to 105 percent of equivalent design speed, and over a range of total to static pressure ratio from 1.62 to 5.07.

Included in this report are turbine design information and turbine performance results in terms of equivalent mass flow, equivalent work, equivalent torque, efficiency, and rotor exit flow angle. Results of a radial survey at design equivalent total to static pressure ratio and rotative speed are also included.

SYMBOLS

A	area, cm^2
Δh	specific work, J/g
N	rotative speed, rpm
p	absolute pressure, N/cm^2
R	gas constant, J/(kg)(K)
R_x	blade reaction, $(W_3^2 - W_2^2)/2\,\Delta h$
r	radius, m
T	absolute temperature, K
U	blade velocity, m/sec
V	absolute gas velocity, m/sec
W	relative gas velocity, m/sec
w	mass flow, kg/sec
α	absolute gas flow angle measured from axial direction, deg
β	relative gas flow angle measured from axial direction, deg
γ	ratio of specific heats

δ ratio of inlet total pressure to U.S. standard sea-level pressure, p_1'/p^*

ϵ function of γ used in relating parameters to those using air inlet conditions at U.S. standard sea-level conditions, $(0.740/\gamma)(\gamma + 1)/2^{\gamma/(\gamma-1)}$

η_L local efficiency (based on local conditions at rotor exit)

η_s static efficiency (based on inlet total to exit static pressure ratio)

η_t total efficiency (based on inlet total to exit total pressure ratio)

θ_{cr} squared ratio of critical velocity at turbine inlet temperature to critical velocity at U.S. standard sea-level temperature, $(V_{cr}/V_{cr}^*)^2$

τ torque, N-m

ω turbine speed, rad/sec

Subscripts:

cr condition corresponding to Mach number of unity

eq equivalent

t rotor tip

u tangential component

1 station at turbine inlet (fig. 5)

2 station at stator exit (fig. 5)

3 station at rotor exit (fig. 5)

Superscripts:

' absolute total state

* U.S. standard sea-level conditions (temperature, 288.15 K; pressure, 10.13 N/cm^2)

TURBINE DESIGN

The turbine used in this experimental investigation was the solid blade version of a turbine designed to drive a two-stage, 10-to-1 pressure ratio compressor with a mass flow of 0.952 kilogram per second, a rotative speed of 70 000 rpm, and a turbine inlet temperature of 1478 K. A list of both the engine design conditions and the equivalent design conditions for this turbine are presented in table I. As discussed in the INTRODUCTION, this turbine was designed for near optimum work factor and solidity. For the solid blade version, minimum tip clearance for hot operation, and the minimum allowable leading and trailing edge thicknesses from a manufacturing standpoint were used.

A total efficiency of 85 percent was selected for the solid blade version of the turbine as being achievable in this size class. An optimum design of a large turbine with the same work factor would be expected to have an efficiency of about 91 to 92 percent in cold-air operation.

The turbine was designed as a single-stage unit with both the stator and rotor blading being untwisted and untapered. An untwisted, untapered design was selected for the cooled turbine design. A desire to maintain similar stator and rotor blade profiles between the uncooled and cooled designs dictated this selection.

Selecting an untwisted design, however, can result in undesirable effects due to incidence, reaction, and radial distribution of specific work as compared to a free-vortex design. In reference 2 a method was presented for calculating the radial distribution of specific work for an untwisted rotor blade design. The results obtained using this method for the subject turbine indicated that no efficiency penalty would occur due to the radial distribution of specific work.

With the aid of reference 3 an analysis was made to determine incidence losses. The design incidence angles are 7.4°, -1.1°, and -14.9° at the hub, mean, and tip, respectively. For these incidence angles the analysis indicated that the blade profile loss would be small. Therefore, any efficiency penalty would be small and was neglected in the design.

Design values of reaction R_x were 0.335, 0.440, and 0.512 at the hub, mean, and tip, respectively. This level of reaction at the tip section could increase the tip clearance loss compared to a lower reaction blade.

For a larger turbine a tip clearance of about 1.5 percent of the blade height could be specified. However, this percentage cannot be scaled to smaller turbines having small blade heights. Engine transient conditions limit the tip clearance in turbines of this size to a level of about 0.25 millimeter, which in this turbine is about 2.4 percent of the blade height.

In order to minimize tip clearance effects, the clearance was obtained by a recess in the outer casing above the rotor blade tips. A previous investigation (ref. 4) indicated that a recessed casing would be the optimum tip clearance configuration.

Table II lists some of the physical parameters for this turbine. An aspect ratio of 1.00 was selected. The solidities of 1.61 and 1.70 for the stator and rotor, respectively, are close to the optimum as defined in reference 6. Using these values of solidity and aspect ratio resulted in 56 stator blades and 59 rotor blades.

Figure 1 shows the velocity diagrams as calculated at the hub, mean, and tip diameters. It can be seen that the stator discharge angle is a constant 74.2° and the rotor discharge angle is a constant 61.9° from hub to tip.

The blade surface velocities at the hub, mean, and tip diameters as calculated from the computer program of reference 7 are shown in figure 2 for the stator and rotor. The figure shows that there was no large diffusion predicted for any of the three blade sections.

Figure 3(a) is a photograph of the stator assembly, and figure 3(b) is a photograph of the rotor and shaft assembly. These photographs show some of the design features of this turbine.

APPARATUS, INSTRUMENTATION, AND TEST PROCEDURE

The apparatus used in this investigation consisted of the subject turbine, an airbrake dynamometer used to absorb and measure the power output of the turbine, an inlet and exhaust piping system including flow controls, and appropriate instrumentation. A schematic of the experimental equipment and instrument measuring stations is shown in figure 4. A cross-sectional view of the turbine is shown in figure 5.

Instrumentation at the turbine inlet (station 1) measured static pressure and total temperature. Static pressures were obtained from eight taps with four on the inner wall and four on the outer wall. The inner and outer taps were located opposite each other at 90° intervals around the circumference at a distance approximately two axial chord lengths upstream of the stator. The temperature was measured with three thermocouple rakes, each containing three thermocouples at the area center radii of three equal annular areas.

At station 3, approximately three axial chord lengths downstream of the rotor, the static pressure, total pressure, total temperature, and flow angle were measured. The static pressure was measured with eight taps with four each on the inner and outer walls. These inner and outer wall taps were located opposite each other at 90° intervals around the circumference. A self-alining probe was used for measurement of total pressure, total temperature, and flow angle.

There were four total temperature rakes, each containing three thermocouples, at station 4 located about 15.7 centimeters downstream from the rotor exit. Temperatures from these rakes were used to calculate a turbine temperature efficiency. This efficiency was used to check the turbine torque efficiency as calculated from torque, speed, and mass flow measurements. Torque efficiency is presented in this report.

The rotational speed of the turbine was measured with an electronic counter in conjunction with a magnetic pickup and a shaft-mounted gear. Mass flow was measured with a calibrated critical flow nozzle. An airbrake dynamometer absorbed the power output of the turbine. Torque was measured by the airbrake, which was supported on trunion gas bearings. The torque load was measured with a commercial strain-gage load cell.

In order to obtain aerodynamic performance, friction torque was added to dynamometer torque. The friction torque from the bearings, seal, and coupling windage was obtained by driving the rotor and shaft over the range of speeds covered in this investigation. In order to eliminate disk windage and blade pumping and churning losses from the friction torque, the turbine cavity was evacuated to a pressure of approximately 0.013 newtons per square centimeter. A friction torque value of 0.285 newton-meter was obtained at equivalent design rotative speed. This value of friction torque corresponds to 6.1 percent of the work obtained at equivalent design rotative speed and pressure ratio.

Data were obtained at nominal inlet total flow conditions of 300 K and 8.27 newtons per square centimeter. The turbine was operated over a range of design equivalent speeds from 0 to 105 percent and over a range of total to static pressure ratios from 1.62 to 5.07.

The turbine was rated on the basis of both total and static efficiency. The total pressures used in determining these efficiencies were calculated from mass flow, static pressure, total temperature, and flow angle from the following equation:

$$p' = p\left\{\frac{1}{2} + \frac{1}{2}\left[1 + \frac{2R(\gamma - 1)}{\gamma}\left(\frac{w\sqrt{T'}}{pA\cos\alpha}\right)^2\right]^{\frac{1}{2}}\right\}^{\gamma/(\gamma-1)}$$

In the calculation of turbine inlet total pressure, the flow angle was assumed to be zero.

RESULTS AND DISCUSSION

Performance results are presented for a 12.766-centimeter-tip-diameter, single-stage, axial-flow turbine. Performance tests were made with air as the working fluid at inlet total conditions of approximately 8.27 newtons per square centimeter and 300 K. The range of speed covered was 0 to 105 percent of equivalent design speed, and the range of total to static pressure ratio covered was 1.62 to 5.07. Experimental results include overall performance in terms of equivalent mass flow, equivalent torque, equivalent specific work, and efficiency. Also included are results of a radial survey conducted at design equivalent total to static pressure ratio and rotative speed.

Mass Flow

Figure 6 shows the variation of equivalent mass flow with total to static pressure ratio. An equivalent mass flow of 0.231 kilogram per second was obtained at equivalent design speed and at the equivalent design total to static pressure ratio of 3.16. This mass flow is about 6.1 percent smaller than the design value of 0.246 kilogram per second. Measurements indicated that the stator throat area was fabricated 5.5 percent smaller than design. However, the rotor throat area was fabricated to design. Therefore, a 5.5. percent flow area mismatch occurred between the stator and rotor, resulting in the turbine operating with mismatched velocity diagrams. This mismatch will be discussed in further detail in the section Turbine Efficiency.

Figure 7 shows the variation of turbine total pressure ratio with turbine inlet total to exit static pressure ratio for lines of constant speed. This figure was included in the report as a reference curve for the reader.

Equivalent Torque

Figure 8 shows the variation of equivalent torque with total to static pressure ratio for lines of constant speed. An equivalent torque value of 4.29 newton-meters was obtained at equivalent design speed and design total to static pressure ratio. This is about 7.6 percent smaller than design. This lower torque value occurred partly because the mass flow was 6.1 percent smaller than design. Since the torque was 7.6 percent smaller than design and the mass flow 6.1 percent smaller than design, it is apparent that the turbine total efficiency would be slightly less than the 85 percent selected for this design. The torque curves show that limiting loading was not reached even though pressure ratios considerably higher than design were obtained.

Rotor Exit Flow Angle

Figure 9 shows the variation of rotor exit flow angle as a function of pressure ratio for lines of constant equivalent speed. The flow angles were measured at the mean radius and from the axial direction. Negative angles indicate a positive contribution to specific work. At design equivalent speed and design total to static pressure ratio of 3.16, the mean radius exit flow angle was about -11°. The velocity diagrams of figure 1 show the turbine was designed for a mean-radius, exit flow angle of -17.5°. Part of this 6.5° difference was caused by the mismatch in flow area between the stator and rotor as discussed earlier. As will be discussed in the next section, the remainder of this difference was caused by a loss core from secondary flows in the stator and rotor. The presence of this loss core caused the rotor exit flow angle to become less negative in the region of the rotor midspan.

Radial Survey Results

Figure 10 shows the results of a radial rotor exit survey obtained at design equivalent speed and total to static pressure ratio. Figure 10(a) shows the radial variation of local efficiency. A loss region extending from a radius ratio of 0.865 to 0.950 can be noted. As noted by the experimental results of reference 8, this midspan loss region was believed to occur as a result of low momentum fluid originating along the hub in the rotor passage being centrifuged toward the outer wall as it moved downstream. The presence of this midspan loss region indicates that in small gas turbines, secondary flows contribute more to the total turbine loss than in larger turbines with aspect ratios of about two or greater.

Figure 10(b) shows the radial variation of absolute rotor exit flow angle with radius ratio. The figure indicates that there was a variation of about 4.5° in flow angle from hub to tip. Figure 10(c) shows the radial variation of total pressure ratio with radius ratio. The region of loss in the midspan region corresponds to the deficit in local efficiency noted earlier.

Turbine Efficiency

A performance map for this turbine is shown in figure 11. The map shows equivalent specific work output $\Delta h/\theta_{cr}$ as a function of the mass flow-speed parameter $\epsilon w \omega/\delta$ for the various equivalent speeds investigated. Lines of constant pressure ratio and efficiency are superimposed. Figure 11(a) shows the performance of the turbine based on total conditions across the turbine. A total efficiency of 83.2 percent was obtained at both equivalent design speed and specific work and equivalent design speed and pressure ratio. This was 1.8 percentage points lower than the 85 percent selected for this design.

Over the range of pressure ratio and speeds investigated, the total efficiency varied from 55 percent near the 30 percent speed line to 84 percent near the 105 percent speed line. Figure 11(b) shows the performance map based on inlet total to exit static pressure ratio. At the condition corresponding to design equivalent speed and specific work, the efficiency was about 76 percent. This compared with a design static efficiency of 77 percent. Since the total efficiency was 83.2 percent for this same operating point, there were 7.2 percentage points in efficiency due to rotor exit kinetic energy. This compares with 8 percentage points in efficiency in terms of kinetic energy from the design velocity diagrams.

Over the range of pressure ratio and speeds investigated, the static efficiency varied from 45 percent near the 30 percent speed line to 77.5 percent near the 105 percent speed line.

In order to evaluate the efficiency potential for this solid blade turbine configuration, it was necessary to evaluate the performance penalties associated with the geometrical anomaly that occurred. As discussed in the section Mass Flow, there was a mismatch between the stator and rotor throat areas.

Reference 9 presents performance results from a larger turbine with a similar mismatch in flow areas. In this case the stator throat area was 9.4 percent smaller than design. This reference turbine had a tip diameter of 24.70 centimeters, a design mass flow of 2.507 kilogram per second, and a design work factor of 1.153. Reference 10 shows that when the stator-rotor flow areas were rematched by opening the stator throat area by 11.4 percent, the efficiency contours on the performance map shifted slightly to the left and a gain of about one point in efficiency resulted.

For the subject turbine a rematch in the stator-rotor flow areas to the design value should also result in a slight shifting to the left of the efficiency contours on the performance map. In this case, however, the improvement in efficiency would be expected to be less than one efficiency point, because as noted from figure 11(a), the variation of efficiency with speed and pressure ratio was small in the region of design speed and work factor. Any improvement in efficiency that would be realized would result from improved incidence and reaction.

SUMMARY OF RESULTS

An experimental investigation was conducted on a 12.766-centimeter-tip-diameter, single-stage, axial-flow turbine over a range of speed and pressure ratio. This turbine was the solid blade version of a compressor drive turbine designed for a 10-to-1 pressure ratio compressor with a turbine inlet temperature of 1478 K. The turbine was designed for near optimum work factor and solidity. The solid blade version was designed for minimum tip clearance, and the minimum leading and trailing edge thicknesses that would be allowable from a manufacturing standpoint. The stator and rotor blading was selected to be nontwisted. The experimental investigation of this configuration was for the purpose of determining baseline aerodynamic performance. The results of this cold-air investigation may be summarized as follows:

1. A total efficiency of 83.2 percent was obtained at both equivalent design speed and pressure ratio and at equivalent design speed and work factor. This was 1.8 percentage points less than the 85 percent selected for this design.

2. A flow area mismatch occurred between the stator and rotor because the stator throat area was fabricated 5.5 percent undersize. A reference turbine with a similar anomaly was used to show that the performance penalty associated with this mismatch would be less than one efficiency point.

3. A radial rotor exit survey obtained at equivalent design speed and total to static pressure ratio showed the presence of a loss core due to secondary flow in the vicinity of the rotor blade midspan. The large extent of this loss region indicates that secondary flows contribute more to the total turbine losses in small turbines than in larger turbines with aspect ratios at about two or greater.

Lewis Research Center,
National Aeronautics and Space Administration,
and
U.S. Army Air Mobility R&D Laboratory,
Cleveland, Ohio, November 14, 1974,
505-04.

REFERENCES

1. Ewen, J. S.; Huber, F. W.; and Mitchell, J. P.: Investigation of the Aerodynamic Performance of Small Axial Turbines. ASME Paper 73-GT-3, Apr. 1973.

2. Slivka, William R.; and Silvern, David H.: Analytical Evaluation of Aerodynamic Characteristics of Turbines with Nontwisted Rotor Blades. NACA TN 2365, 1951.

3. Ainley, D. G.; and Mathieson, C. G. R.: A Method of Performance Estimation for Axial-Flow Turbines. R. & M. No. 2974, British A.R.C., 1951.

4. Kofskey, Milton G.: Experimental Investigation of Three Tip-Clearance Configurations over a Range of Tip Clearance Using a Single-Stage Turbine of High Hub-to Tip Radius Ratio. NASA TM X-472, 1961.

5. Rogo, Casimir: Experimental Aspect Ratio and Tip Clearance Investigation on Small Turbines. SAE Paper 680448, May 1968.

6. Miser, James W.; Stewart, Warner L.; and Whitney, Warren J.: Analysis of Turbomachine Viscous Losses Affected by Changes in Blade Geometry. NACA RM E56F21, 1956.

7. Katsanis, Theodore: FORTRAN Program for Calculating Transonic Velocities on a Blade-to-Blade Stream Surface of a Turbomachine. NASA TN D-5427, 1969.

8. Kofskey, Milton G.; and Allen, Hubert W.: Investigation of a 0.6 Hub-Tip Radius Ratio Transonic Turbine Designed for Secondary-Flow Study. IV - Rotor Loss Patterns as Determined by Hot-Wire Anemometers with Rotor Operating in a Circumferentially Uniform Inlet Flow Field. NACA RM E58B27, 1958.

9. Kofskey, Milton G.; Roelke, Richard J.; and Haas, Jeffrey E.: Turbine for a Low-Cost Turbojet Engine. I - Design and Cold-Air Performance. NASA TN D-7625, 1974.

10. Kofskey, Milton G.; Nusbaum, William J.; and Haas, Jeffrey E.: Turbine for Ordnance Turbojet Engine. II - Cold-Air Performance with Opened Stator. NASA TN D-7626, 1974.

TABLE I. - TURBINE DESIGN CONDITIONS

Parameter	Engine	Equivalent
Turbine inlet temperature, T_1', K	1478	288.2
Turbine inlet pressure, p_1', N/cm^2	91.2	10.1
Mass flow rate, w, kg/sec	0.952	0.246
Rotative speed, N, rpm	70 000	31 460
Specific work, Δh, J/g	307.3	62.1
Torque, τ, N-m	37.98	4.64
Power, kW	280	15
Total to total pressure ratio, p_1'/p_3'	2.57	2.77
Total to static pressure ratio, p_1'/p_3	2.92	3.16
Total efficiency, η_t	0.85	0.85
Work factor, $\Delta V_u/U$	1.67	1.67

TABLE II. - TURBINE PHYSICAL PARAMETERS

Parameter	Stator	Rotor
Actual chord, cm	1.051	1.051
Axial chord, cm	0.721	0.968
Leading edge radius, cm	0.102	0.059
Trailing edge radius, cm	0.020	0.025
Radius, cm		
Hub	5.331	5.331
Mean	5.857	5.857
Tip	6.383	6.383
Blade height, cm	1.051	1.051
Solidity	1.61	1.70
Aspect ratio	1.00	1.00
Number of blades	56	59
Radius ratio	0.835	0.835

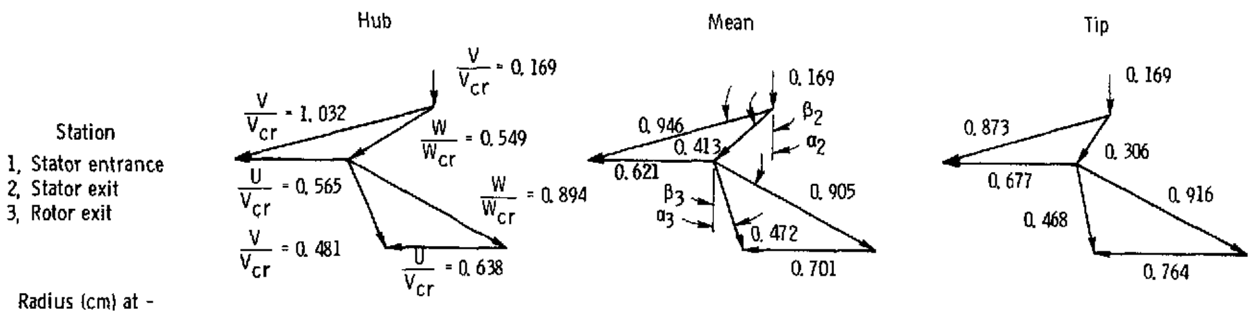

	Hub	Mean	Tip
Radius (cm) at -			
Station 1	5.33	5.86	6.38
Station 2	5.33	5.86	6.38
Station 3	5.33	5.86	6.38
α_2, deg	74.2	74.2	74.2
β_2, deg	56.7	48.2	34.4
α_3, deg	-23.3	-17.5	-11.6
β_3, deg	-61.9	-61.9	-61.9

Figure 1. - Design velocity diagrams.

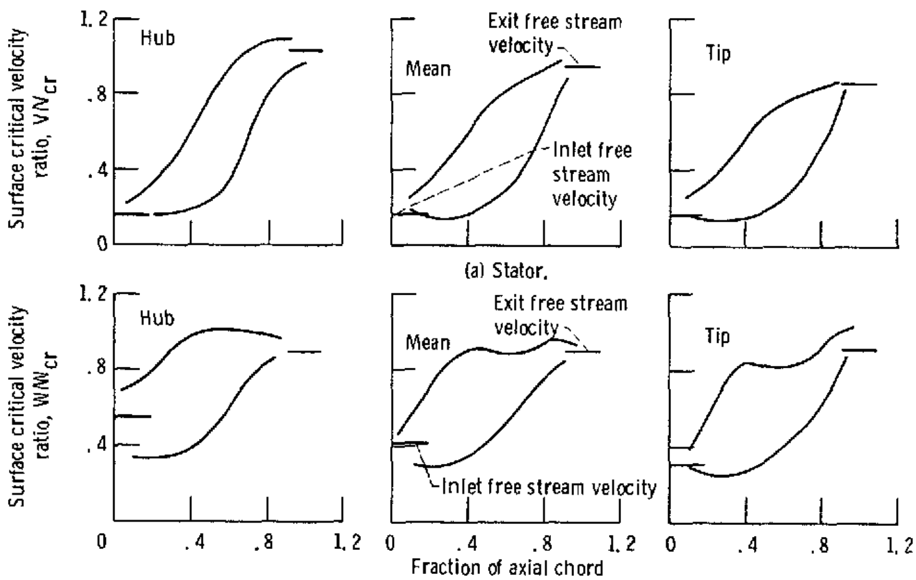

(a) Stator.

(b) Rotor.

Figure 2. - Design blade surface velocity distributions at hub, mean, and tip.

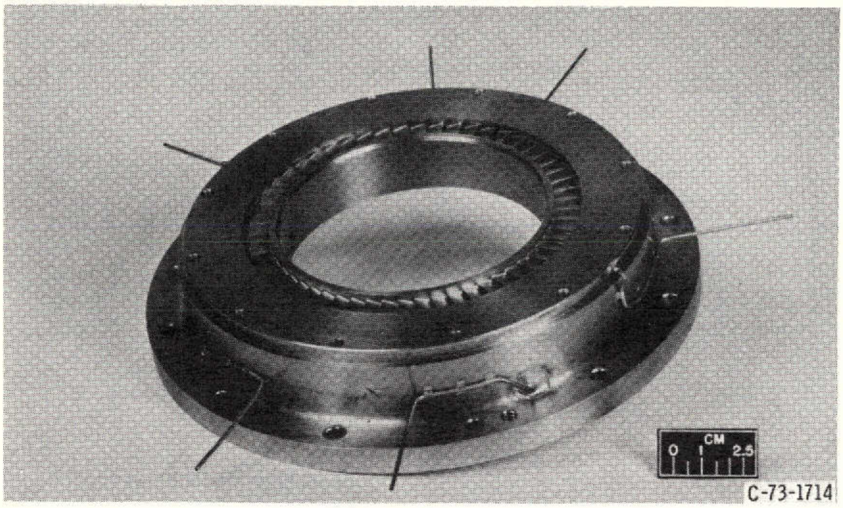

(a) Stator assembly.

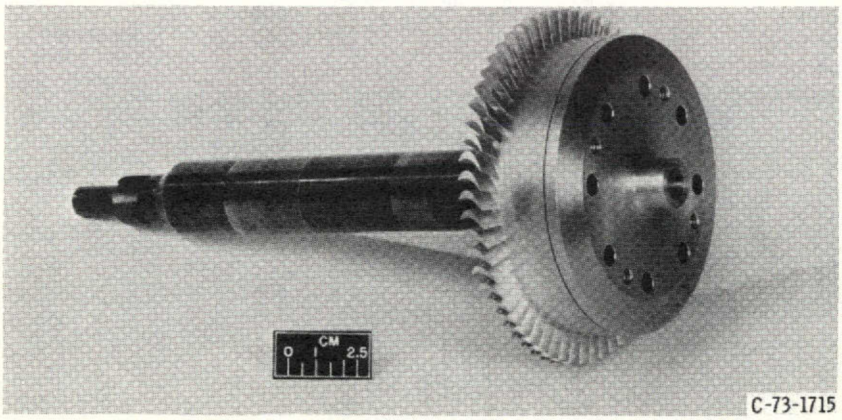

(b) Rotor and shaft assembly.

Figure 3. - Turbine test hardware.

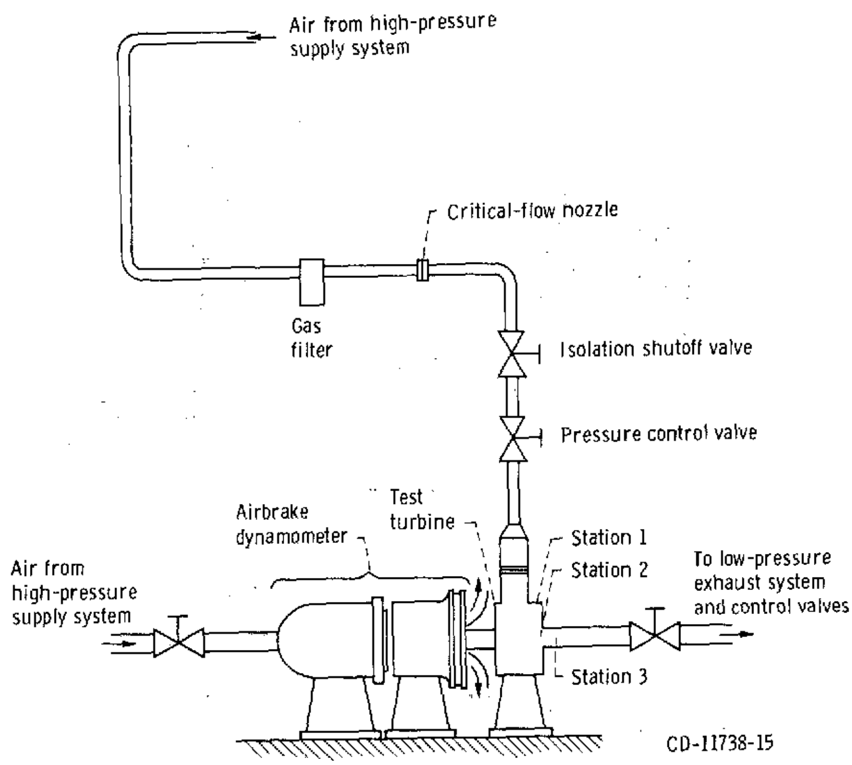

Figure 4. - Experimental equipment.

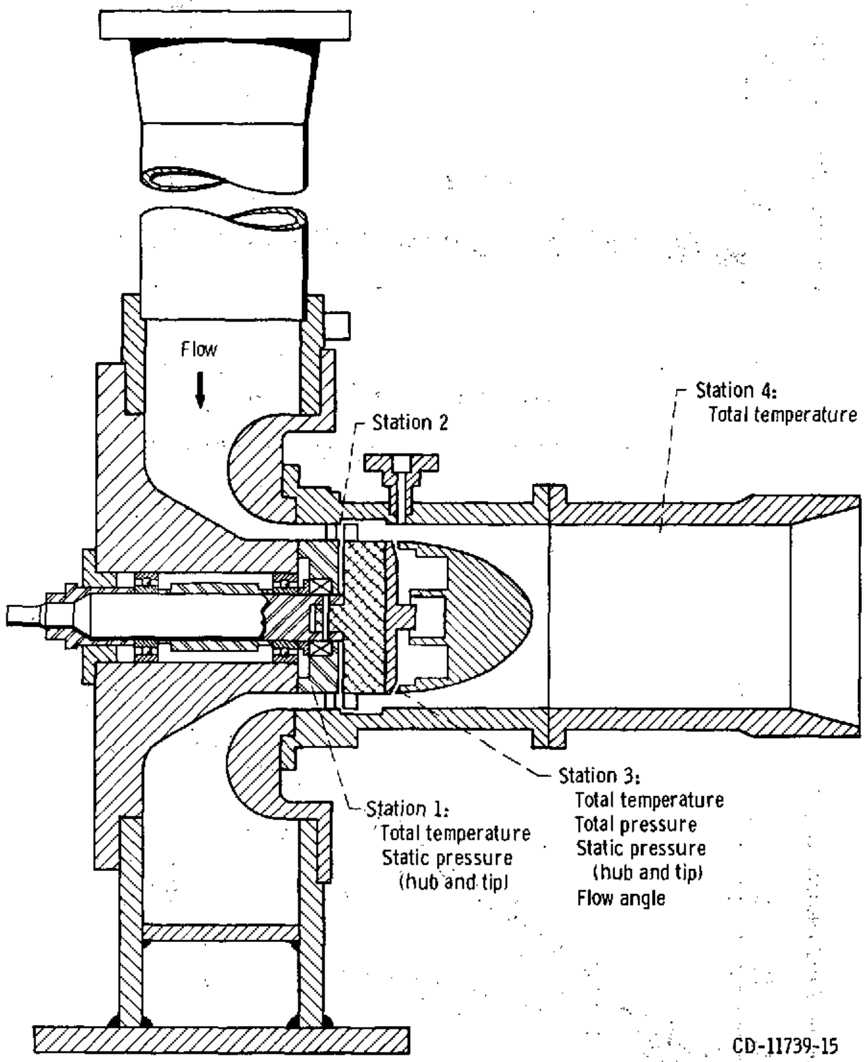

Figure 5. - Schematic of turbine.

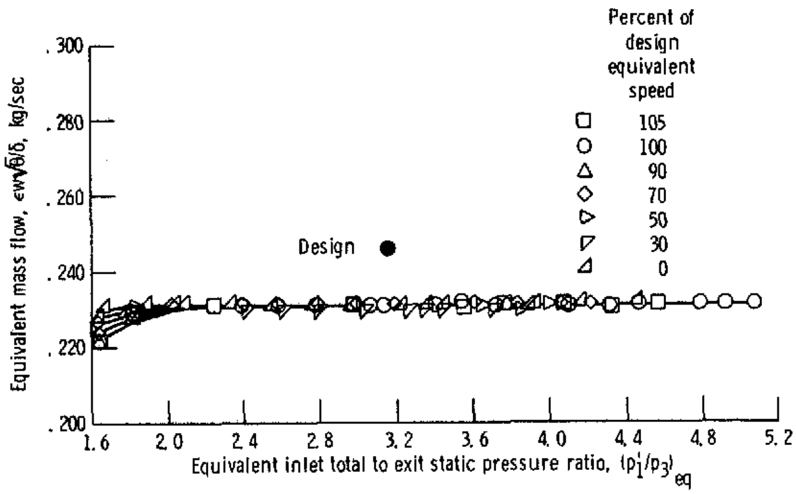

Figure 6. - Variation of mass flow with pressure ratio and speed.

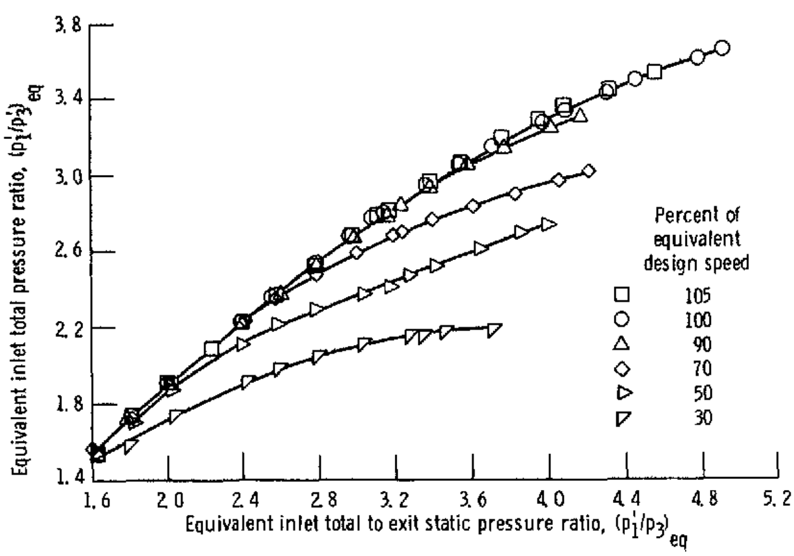

Figure 7. - Variation of total pressure ratio with total to static pressure ratio.

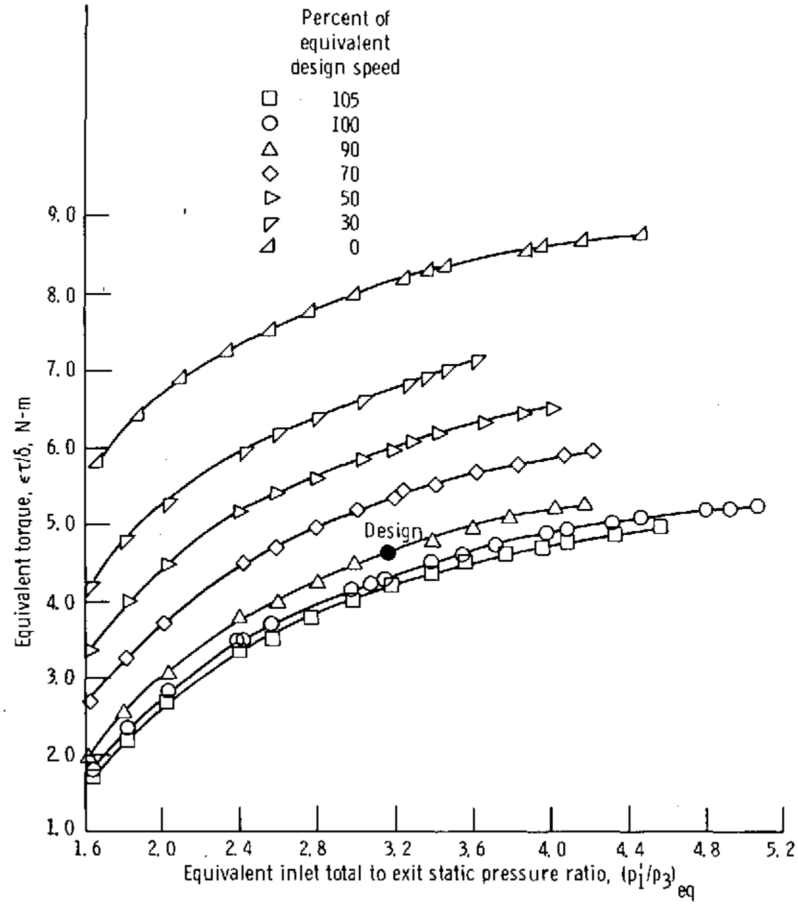

Figure 8. - Variation of torque with pressure ratio and speed.

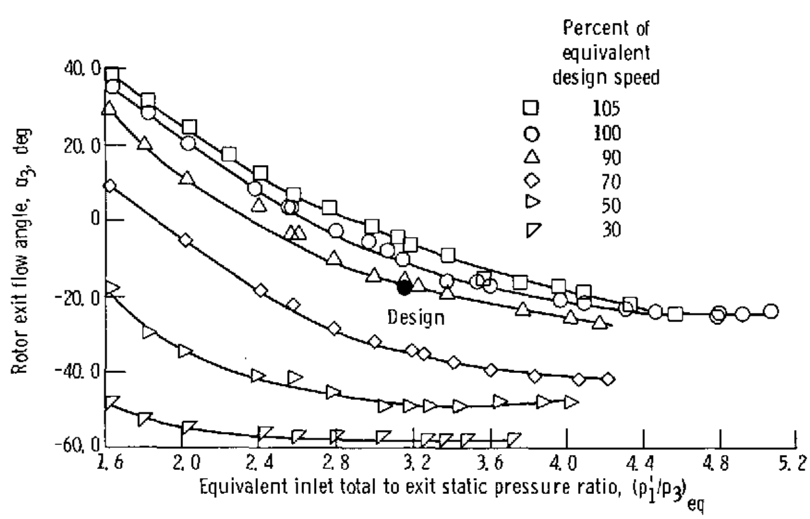

Figure 9. - Variation of rotor exit flow angle with pressure ratio and speed.

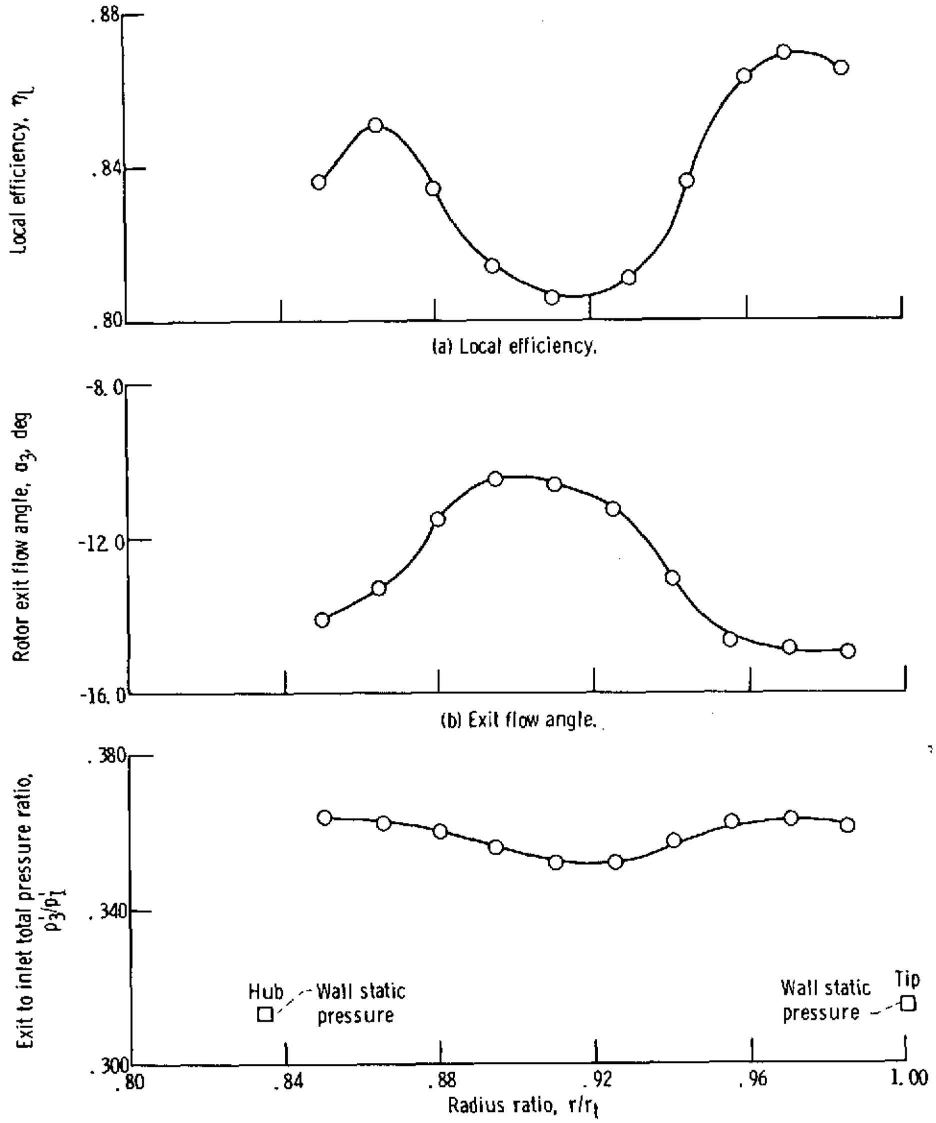

(c) Exit to inlet total pressure ratio.

Figure 10. - Variation of local efficiency, flow angle, pressure ratio with radius ratio at and design speed and pressure ratio.

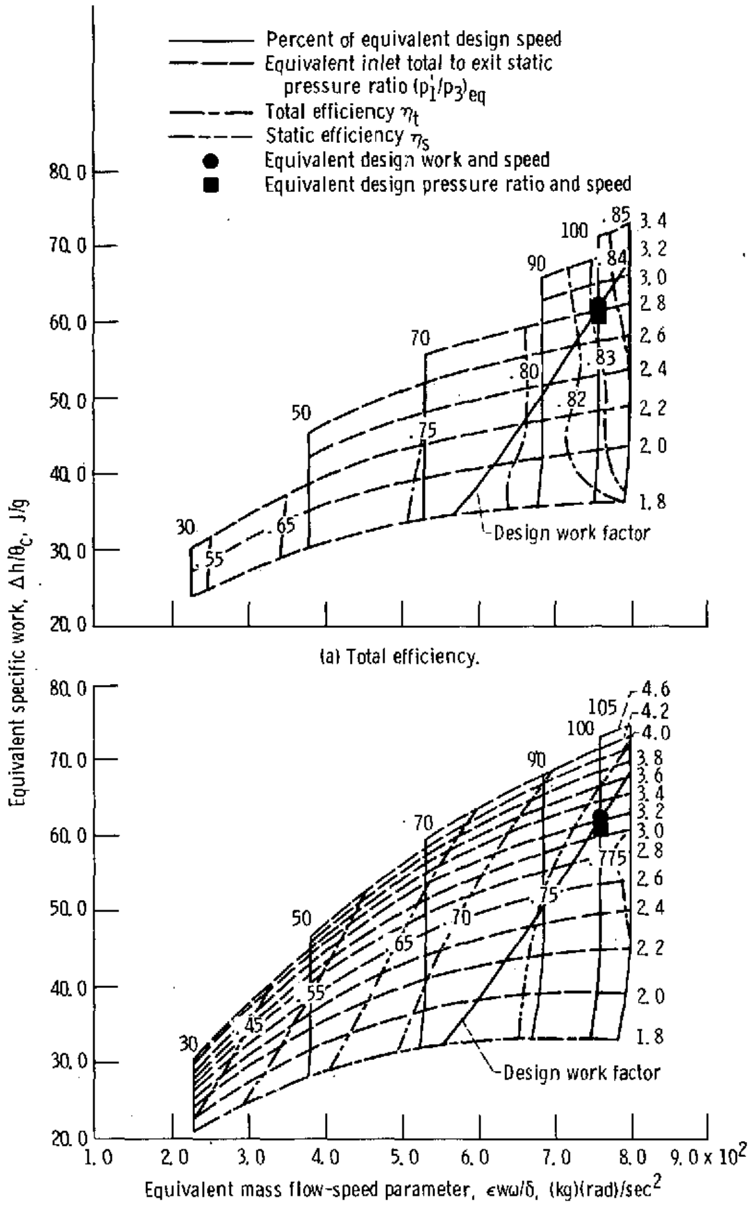

(a) Total efficiency.

(b) Static efficiency.

Figure 11. - Overall total performance map.